Electronic Supporting Information: Microscopic time-resolved imaging of singlet oxygen by delayed fluorescence in living cells

Marek Scholz, Roman Dědic, and Jan Hála

July 20, 2017

1 SOFDF kinetics according to the simple model

The kinetics of PS T_1 states, $^1O_2$, and SOFDF calculated according to the model (3) for a water solution and cellular environment are displayed in the figure ESI-1.

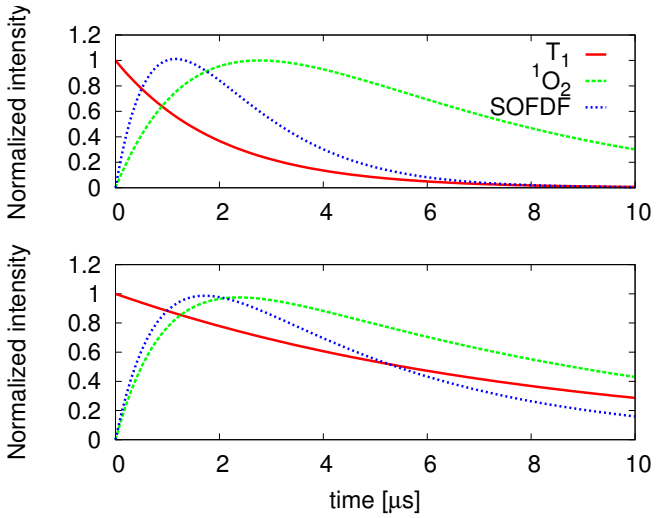

Figure ESI-1: Normalized kinetics of T_1 states, $^1O_2$, and SOFDF computed according to the model (3). Top: $\tau_\Delta = 4\,\mu s$ and $\tau_T = 2\,\mu s$, which corresponds to the solution of $AlPcS_4$ in water. Bottom: $\tau_\Delta = 1\,\mu s$ and $\tau_T = 8\,\mu s$, which roughly reflects the situation which may be encountered in cells.

2 Validity of the model

There are two major inaccuracies related to the simple SOFDF model (3): i) There is not a single $^1O_2$ and T_1 lifetime in the complex cellular environment, but a distribution of lifetimes. ii) the model neglects the process of SOFDF as one of the quenching channels of $^1O_2$ and T_1 states. Regarding the point i), the $^1O_2$ phosphorescence kinetics recorded from cells have been commonly and satisfactorily fitted by two exponentials thus assuming one effective $^1O_2$ lifetime and one T_1 lifetime.[37,38,41,50,51] The same applies for our work. The point ii) is discussed in the following paragraph.

The local subcellular PS concentration in cells can be quite large and the concentrations of excited states may reach relatively high levels, which could lead to a remarkable effect of the $^1O_2$ feedback on the kinetics and τ_Δ, τ_T lifetimes. To

estimate the influence of $^1O_2$-feedback on the kinetics of excited states, we solve the set of differential equations

$$\begin{aligned}\frac{\mathrm{d}}{\mathrm{d}t}[\mathrm{T}_1] &= -k_{\mathrm{T}\Delta}[\mathrm{O}_2][\mathrm{T}_1] - k_{0\mathrm{T}}[\mathrm{T}_1] - (1-\Phi'_{\mathrm{T}})k_{\mathrm{SOF}}[^1\mathrm{O}_2][\mathrm{T}_1]\\ \frac{\mathrm{d}}{\mathrm{d}t}[^1\mathrm{O}_2] &= \quad k_{\mathrm{T}\Delta}[\mathrm{O}_2][\mathrm{T}_1] - k_{0\Delta}[^1\mathrm{O}_2] - k_{\mathrm{SOF}}[^1\mathrm{O}_2][\mathrm{T}_1]\\ [\mathrm{O}_2] &= [\mathrm{O}_2]_0 - [^1\mathrm{O}_2]\end{aligned} \tag{ESI-1}$$

with initial conditions $[\mathrm{T}_1](t=0) = [\mathrm{T}_1]_0$ and $[^1\mathrm{O}_2](t=0) = 0$. $k_{\mathrm{T}\Delta}$ is the bimolecular rate of $^1O_2$ photosensitization from PS triplets, $k_{0\mathrm{T}}$ is the oxygen-independent rate of PS triplet deactivation, Φ'_{T} is the fraction of PS molecules which undergo ISC again after the $^1O_2$-feedback,* k_{SOF} is the bimolecular rate of the $^1O_2$-feedback reaction, $k_{0\Delta}$ is the $^1O_2$ deactivation rate by the solvent+biomolecules, and $[\mathrm{O}_2]_0$ is the initial concentration of the ground state oxygen. The parameters in the equations are dependent on the solvent/environment, particularly on the diffusion coefficient of oxygen ($\approx 2-4\times10^{-6}\,\mathrm{cm^2s^{-1}}$ in cells, $\approx 2\times10^{-5}\,\mathrm{cm^2s^{-1}}$ in water[40]). The figure ESI-2 compares the calculated kinetics for cell samples with $[\mathrm{T}_1]_0 = 1$, 100 and 500 µM, using parameter values $k_{\mathrm{T}\Delta} = 3\times10^8\,\mathrm{M^{-1}s^{-1}}$, $k_{\mathrm{SOF}} = 1.5\times10^9\,\mathrm{M^{-1}s^{-1}}$ (the maximal conceivable value approximating the diffusion limit, an overestimation of the real value), $k_{0\mathrm{T}} = 1\times10^4\,\mathrm{s^{-1}}$, $k_{0\Delta} = 6.6\times10^5\,\mathrm{s^{-1}}$, $\Phi'_{\mathrm{T}} = 0.4$, and $[\mathrm{O}_2] = 280\,\mu\mathrm{M}$. The displayed kinetics have been fitted with two exponentials in the case of SOFDF and $^1O_2$, and with one exponential in the case of T_1 kinetics.

The influence of the $^1O_2$ feedback is still relatively small for $[\mathrm{T}_1]_0 = 100\,\mu\mathrm{M}$. However, significant changes are observed for $[\mathrm{T}_1]_0 = 500\,\mu\mathrm{M}$. This is particularly visible in the $^1O_2$ kinetics, which no longer can be fitted by two exponentials. The rise-time of $^1O_2$ kinetics is faster, which is due to the quenching of $^1O_2$ by the feedback mechanism. This lifetime shortening is reflected also in the SOFDF kinetics rise-time. The SOFDF kinetics still can be quite satisfactorily fitted with two exponentials even at $[\mathrm{T}_1]_0 = 500\,\mu\mathrm{M}$. Moreover, the rise-time of SOFDF is still a good predictor of the $^1O_2$ rise-time ($^1O_2$ lifetime): The $^1O_2$ rise-time drops from 1.5 µs to 0.7 µs when $[\mathrm{T}_1]_0$ changes from 1 µM to 500 µM. The SOFDF rise-time drops as well from 1.3 µs to 0.6 µs. If we assume $k_{\mathrm{SOF}} = k_{\mathrm{T}\Delta} = 3\times10^8\,\mathrm{M^{-1}s^{-1}}$, which is a smaller and probably more realistic value of k_{SOF}, then the differences between the kinetics for $[\mathrm{T}_1]_0 = 1\,\mu\mathrm{M}$ and $[\mathrm{T}_1]_0 = 500\,\mu\mathrm{M}$ are only subtle (data not shown), with $^1O_2$ lifetimes 1.5 µs and 1.1 µs, respectively, and SOFDF rise-times 1.3 µs and 1.0 µs, respectively. The precise value of k_{SOF} is not known, but it has been shown that it is approximately in the order of the $k_{\mathrm{T}\Delta}$ rate.[19,21] The discussion in this paragraph demonstrates that the SOFDF simple model can be used for approximate estimation of the cellular excited state lifetimes even in the case that $^1O_2$ feedback is not a negligible channel of $^1O_2$ and T_1 deactivation.

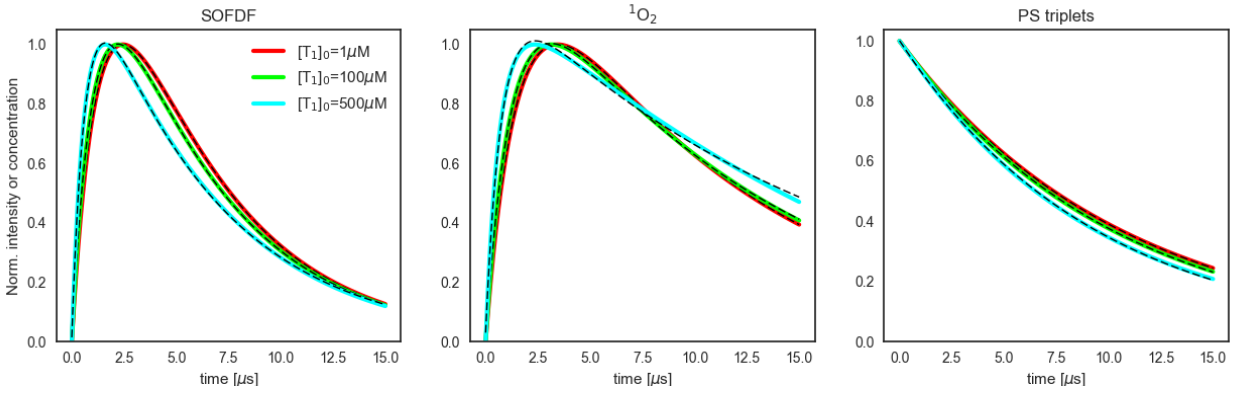

Figure ESI-2: Kinetics when taking into account the $^1O_2$-feedback mechanism as a non-negligible quenching channel of $^1O_2$ and T_1. The kinetics for three different initial T_1 concentations are displayed. The calculated kinetics (solid lines) were fitted with one or two exponentials (dashed lines).

3 Comparison of SOFDF intensity and $^1O_2$ phosphorescence intensity

The emission rate of SOFDF photons per unit volume can be calculated as

$$I_{\mathrm{SOFDF}} = \Phi'_{\mathrm{F}} k_{\mathrm{SOF}}[^1\mathrm{O}_2][\mathrm{T}_1]\,,$$

*Φ'_{T} is not necessarily equal to Φ_{T}, because the repopulated S_1 after the $^1O_2$-feedback process is in close proximity of oxygen molecule, which may perturb the S_1 state.

where k_{SOF} is the bimolecular rate of the $^1O_2$ feedback reaction ($T_1 + {}^1O_2 \rightarrow S_1 + {}^3O_2$) and Φ'_F is the quantum yield of fluorescence from the repopulated S_1 of the PS.

On the other hand, the emission rate of $^1O_2$ phosphorescence photons in water is

$$I_{^1O_2} = k_r[^1O_2] = 0.11\,s^{-1}[^1O_2]\,,$$

where k_r is the radiative rate (the $^1O_2$ radiative rate in lipid-based environment is larger, around $1\,s^{-1}[^1O_2]$)[38,69,70]

The ratio of SOFDF rate and $^1O_2$ phosphorescence rate is

$$R = \frac{I_{SOFDF}}{I_{^1O_2}} = \Phi'_F \frac{k_{SOF}}{k_r}[T_1]\,. \qquad \text{(ESI-2)}$$

It has been shown in our previous work that $k_{SOF}\Phi'_F/\Phi_F > 1\times10^9\,M^{-1}s^{-1}$ for $TPPS_4$ in water and even larger for $AlPcS_4$.[19] Therefore $k_{SOF} > 1\times10^9\,M^{-1}s^{-1}$ when assuming $\Phi'_F = \Phi_F$, *i.e.* the fluorescence yield from the repopulated S_1 is identical to the yield from the directly light-excited S_1. Such rate constants are comparable to those of $^1O_2$ photosensitization from the PS triplets. The diffusion constants in cells are $5-10\times$ smaller than in water[40,67] resulting in slower rates of bimolecular processes. For further calculations, we therefore assume that $k_{SOF} = 2\times10^8\,M^{-1}s^{-1}$ in cells The fluorescence quantum yield of $AlPcS_4$ in water is large, $\Phi_F = 0.58$.[68] For simplicity, we assume the same value for the cellular environment. These values enable us to calculate the ratio R for a given T_1 concentration.

For $[T_1] = 1\,\mu M$, the equation gives $R = 1.1\times10^3$. Hence the rate of SOFDF is three orders of magnitude larger than the rate of $^1O_2$ phosphorescence emission. This ratio scales proportionally with the concentration of PS triplets. It can be shown that a significant fraction of the PS molecules can end up in the triplet state when the sample is irradiated by a focused pulsed laser (pages 63–66 in[71]). Given the high local concentrations of PS inside the cells and lysosomes,[37] it is evident that the SOFDF signal can be several orders of magnitude stronger than the $^1O_2$ phosphorescence.† Indeed, the microscopic experiments in cells incubated with 100 µM $TPPS_4$ showed that the SOFDF quantum yield was around 10^{-4},[20] whereas the $^1O_2$ phosphorescence quantum yield in water-based biological systems is smaller than 10^{-6}.[70]

4 DF imaging of a water/grease system

Vaselinum grease (Valinka) on a glass slide was mixed with a small amount of 100 µM $AlPcS_4$ water solution (optionally with 10 mM NaN_3) and covered by a cover slip. This sample provides a simple model of micrometric photosensitizer-loaded domains surrounded by a non-luminescent environment.

In the water/grease phase separated system, the iCCD gate-width was set to 200 ns and a sequence of 50 DF images was acquired with the delay gradually increasing from 180 ns to 10 180 ns with a 200 ns increment. The acquisition time of each image is 2.5 seconds. No significant photobleaching occurs during the course of the acquisition due to the excellent photostability of $AlPcS_4$.

Figure ESI-3 displays several DF images recorded at different time-intervals after the excitation pulse. The graph shows the averaged DF intensity in the droplet as a function of the gate-delay. The DF image sequence and the graph clearly show that the DF kinetics exhibits a rise-decay shape which is typical for the SOFDF mechanism. The kinetics was fitted by two exponentials with decay-time $\tau_1 = (1.6\pm0.3)$ µs and rise-time $\tau_2 = (0.7\pm0.2)$ µs.

The DF kinetics is quenched and loses the rise-decay character typical for SOFDF in the droplets with addition of 10 mM of the specific $^1O_2$ quencher NaN_3. It follows approximately a single exponential decay with lifetime of (1.5 ± 0.3) µs. This indicates that DF is produced mainly by the SOFDF mechanism in the unquenched samples. In contrary, the DF decay- and rise-times are prolonged to (2.0 ± 0.2) µs and (0.8 ± 0.2) µs, respectively, in droplets formed by $AlPcS_4$ dissolved in D_2O (data not shown) due to the longer $^1O_2$ lifetime in D_2O. It is a further proof of the SOFDF mechanism.[19] The results obtained in the phase-separated systems demonstrate that the setup is able to acquire time-resolved images of DF in H_2O-based environment with microscopic spatial resolution.

5 Spectrum of DF and PF in cells

A 355 nm pulsed Q-switched laser (Changchun New Industries Optoelectronics Technology 3 kHz, 9 ns pulse duration) was used for excitation to measure the DF and PF spectra from individual cells. A specific cell is imaged on the entrance slit of the spectrograph. In x-dimension, the image is dispersed into the spectral image by the diffraction grating and

†The decay-time of SOFDF is generally shorter than the decay-time of $^1O_2$-phosphorescence. If $\tau_T \ll \tau_\Delta$ (e.g. in certain organic solvents), the SOFDF decay-time is much shorter than the $^1O_2$ phosphorescence decay-time and the SOFDF integral intensity drops. However, this is not the case of cells, where $\tau_T > \tau_\Delta$. The SOFDF-based detection of $^1O_2$ is promising mainly in systems with prolonged PS triplet lifetimes, such as oxygen-depleted samples and samples with high viscosity (*e.g.* the intracellular environment).

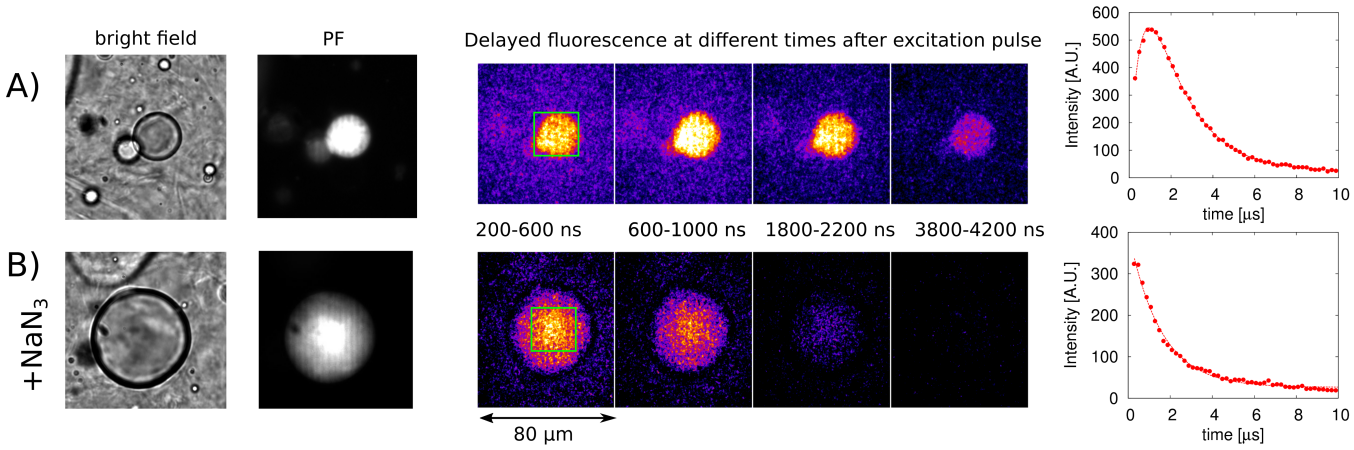

Figure ESI-3: Time-resolved DF images of $AlPcS_4$-containing water droplets in grease at selected time-intervals after the excitation pulse. A: H_2O droplets, B: H_2O+NaN_3 droplets. The kinetics in the graphs on the right were obtained by averaging the DF intensity in the area defined by the green rectangle across the whole DF image-sequence.

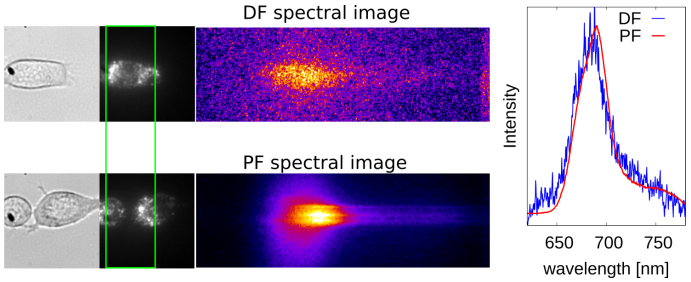

Figure ESI-4: DF (top) and PF spectra (bottom) from cells incubated with $AlPcS_4$ excited at 355 nm. The green rectangle shows the area imaged on the entrance slit of the imaging spectrograph.

recorded by the iCCD. The final spectrum is obtained by summation of the spectral image in the y-dimension. In order to obtain the whole $AlPcS_4$ emission spectrum from individual cells, the 355 nm laser was used for excitation together with a 400 nm longpass dichroic mirror and filter. For the DF spectrum, the signal was accumulated for twenty thousands laser pulses (ca. ten seconds) with a 600 ns delay and 5 µs gate-width. The PF spectrum can be recorded by putting the camera into an internal-trigger mode, which cancels the synchronization of the laser and gate. Under such conditions, the camera collects both PF and DF, but PF is several orders of magnitude stronger.

Figure ESI-4 shows a comparison of the DF and PF spectra recorded microscopically from individual cells. The green rectangle shows the area of the sample which was imaged on the entrance slit of the spectrograph. There is no significant difference between the DF and PF spectra. The slight mismatch is caused by the broad entrance slit (in the case of DF image, the brightest part of the cell is on the left side of the slit, whereas in the case of PF the brightest part is on the right side of the slit.)

6 Relocalization of $AlPcS_4$ in cells

The figure ESI-5-A shows that the time of the increase in PF intensity nicely correlates with the drop in the DF intensity during the light-induced relocalization. On the other hand, the figure ESI-5-B demonstrates that the PF intensity increase is not exhibited in all cell samples, whereas the DF drop is always present. Figure ESI-5-C shows that the relocalization to the nucleus proceeds also in dark.

7 DF kinetics during relocalization measured by iCCD

The DF kinetics measured from ensemble of cells by the photomultiplier suffers from a background signal at short times which interferes with the rise-part of the SOFDF kinetics especially when SOFDF becomes weaker after the $AlPcS_4$ relocalization. DF kinetics measured by iCCD from individual cells provide weaker initial background signal and enable

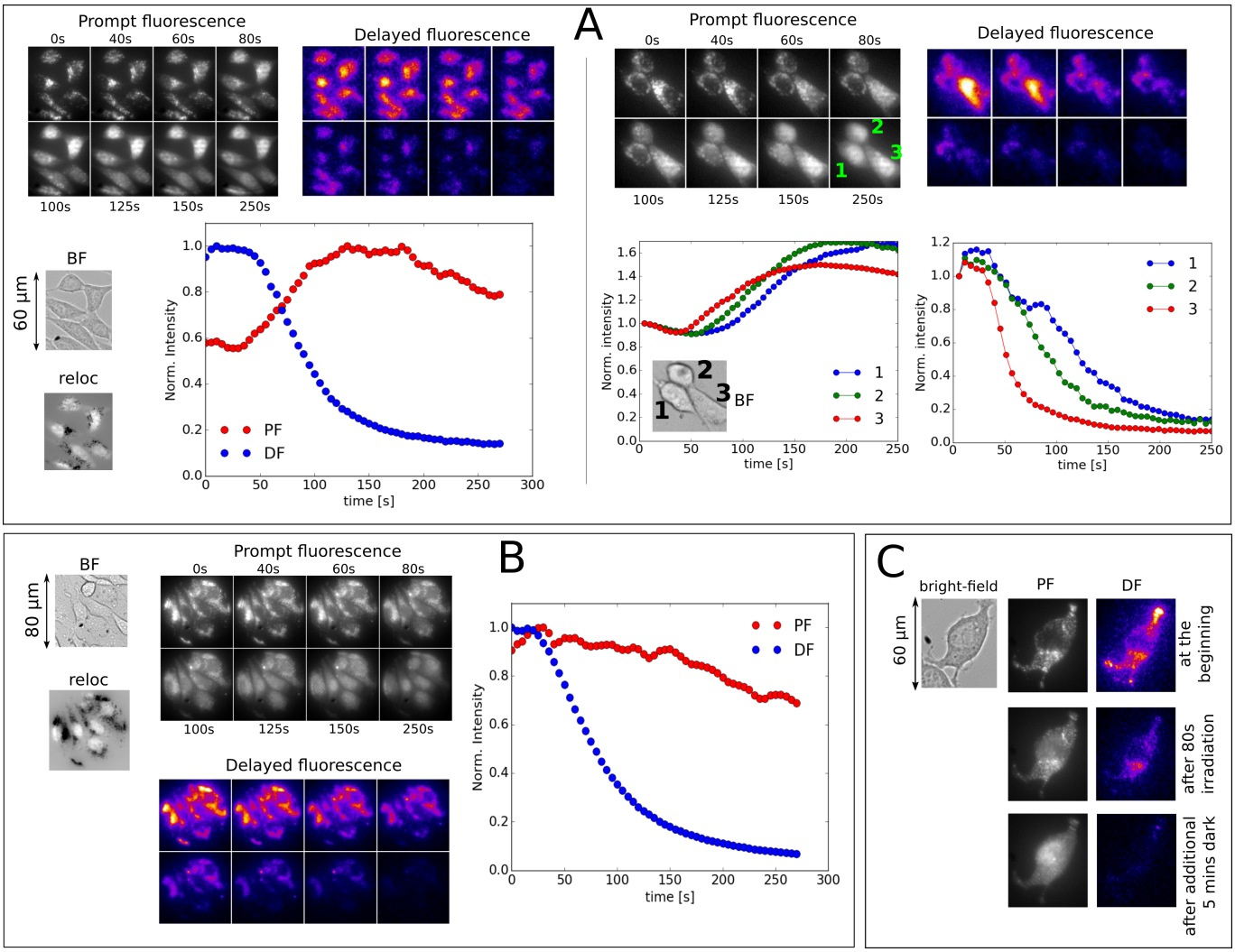

Figure ESI-5: **A:** PF and DF images of cells at different times during the laser irradiation. The graphs show the overall average PF and DF intensity in the cells as a function of irradiation time. The image labeled "reloc" shows the difference image between the final and initial PF image. The PF intensity grows during relocalization in these samples and the DF drop nicely correlates in time with the PF increase. **B:** Cell images showing that PF sometimes decreases upon relocalization instead of growing. **C:** PF and DF images documenting that relocalization to the nucleus proceeds also in dark.

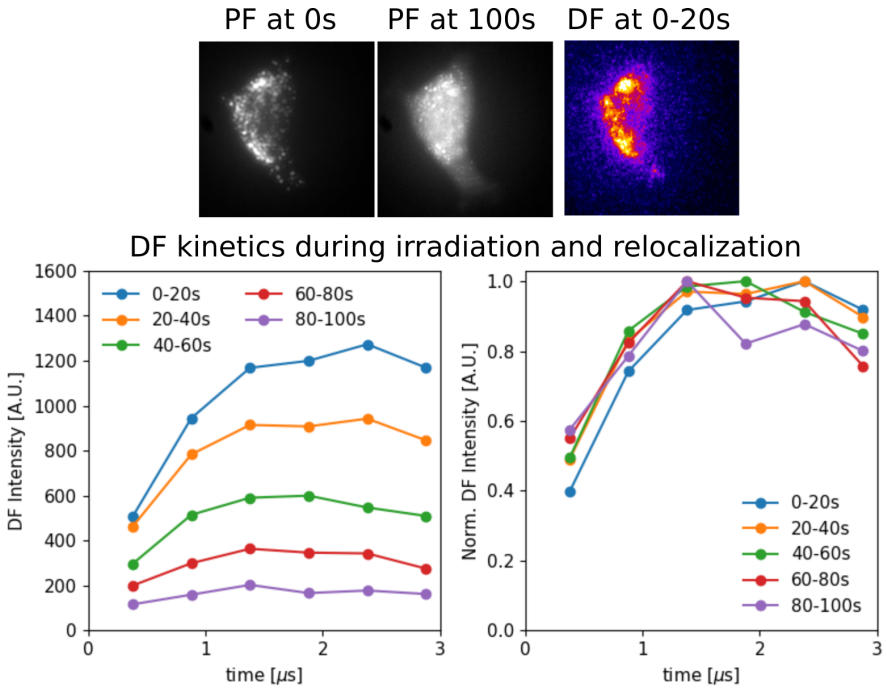

Figure ESI-6: Bottom: Kinetics from a single cell detected by iCCD during continuous irradiation. The PF images of the cell at the beginning and after 100 s irradiation are shown at the top together with the DF image in the time interval 0-20 s obtained by summation of the DF time-resolved sequence.

us to better resolve the rise-part of the SOFDF kinetics. The figure ESI-6 demonstrates that the DF rise-part can be detected even after relocalization of $AlPcS_4$ from lysosomes.

8 D_2O and NaN_3 effect on DF kinetics

The figure ESI-7 shows that the presence of D_2O leads to a prolongation of SOFDF lifetimes, whereas NaN_3 quenches the SOFDF emission.

9 Lifetime imaging

Pseudo-lifetime images can be obtained by comparing the images from DF time-resolved sequences. For example, the DF image at time-window 0.6 µs–2.6 µs can be divided by the 4.6 µs–6.6 µs image pixel by pixel. In the resulting pseudo-lifetime image, the colour codes the ratio of the pixel values, *i.e.* the rate of the DF decay. Figure ESI-8 shows such ratio images for cells treated by PBS-H_2O, PBS-D_2O, and PBS-H_2O+NaN_3. The images clearly show that the DF decay rate is the fastest for the PBS-H_2O+NaN_3 and the smallest for the the PBS-D_2O treated cell, as expected. The ratio values are rather uniform over the analyzed regions of the cells, not showing any significant intracellular or inter-cellular differences. Interestingly, when the lifetime-images are calculated from the two consecutive sequences in the PBS-H_2O+NaN_3 sample, they show that the decay is significantly faster in the second sequence. This is in accord with the observation from the section 4.7 of the article, where it was shown that the NaN_3 quenches SOFDF much stronger after the initial 15 s of irradiation.

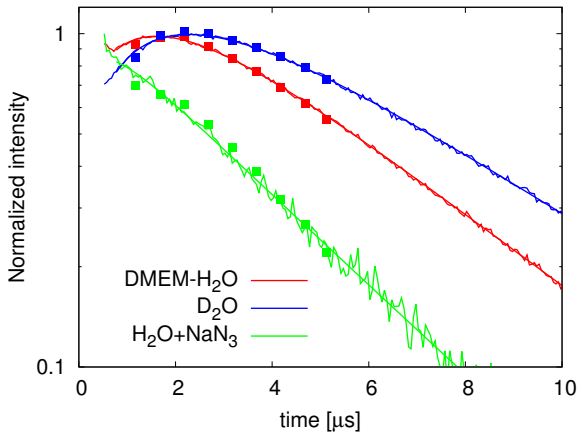

Figure ESI-7: The sum of DF kinetics over all the investigated experimental spots in the given medium (DMEM/H_2O in red, D_2O green, H_2O+NaN_3 in blue) as measured by the iCCD (squares) and photomultiplier (lines) Only the CCD data in time-interval 1 µs–5 µs are displayed since this time-interval provides the largest statistical set.

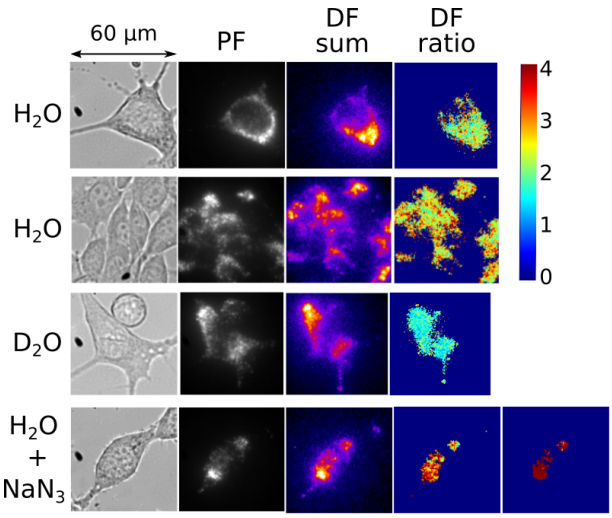

Figure ESI-8: DF ratio images obtained by dividing the 0.6 µs–2.6 µs image by the 4.6 µs–6.6 µs image pixel by pixel. Red colour corresponds to the fastest decay rate and blue-green colours to slow decay rates. For the sample held in H_2O+NaN_3, ratio images derived from two consecutive image-sequences are displayed, showing that the decay is faster in the second sequence, i.e. after 20 s irradiation.